RESEARCH ARTICLE

GCB-BIOENERGY
BIOPRODUCTS FOR A SUSTAINABLE BIOECONOMY

WILEY

Site impacts nutrient translocation efficiency in intraspecies and interspecies miscanthus hybrids on marginal lands

Elena Magenau[1] | John Clifton-Brown[2] | Danny Awty-Carroll[2] | Chris Ashman[2] | Andrea Ferrarini[3] | Mislav Kontek[4] | Enrico Martani[3] | Kevin Roderick[2] | Stefano Amaducci[3] | Chris Davey[2] | Vanja Jurišić[4] | Jason Kam[5] | Luisa M. Trindade[6] | Iris Lewandowski[1] | Andreas Kiesel[1]

[1]Institute of Crop Science, Biobased Resources in the Bioeconomy, University of Hohenheim, Stuttgart, Germany

[2]Department of Biological, Environmental and Rural Sciences, Aberystwyth University, Aberystwyth, Ceredigion, UK

[3]Department of Sustainable Crop Production, Università Cattolica del Sacro Cuore, Piacenza, Italy

[4]Department of Agricultural Technology, Storage and Transport, University of Zagreb, Zagreb, Croatia

[5]Terravesta, Lincoln, UK

[6]Plant Breeding, Wageningen University and Research, Wageningen, The Netherlands

Correspondence
Elena Magenau, Institute of Crop Science, Biobased Resources in the Bioeconomy, University of Hohenheim, 70599 Stuttgart, Germany.
Email: elena.magenau@uni-hohenheim.de

Abstract

Miscanthus, a C_4 perennial rhizomatous grass, is capable of growing in varied climates and soil types in Europe, including on marginal lands. It can produce high yields with low nutrient inputs when harvested after complete senescence. Senescence induction and rate depend on complex genetic, environmental, and management interactions. To explore these interactions, we analysed four miscanthus hybrids (two novel seed-based hybrids, GRC 3 [*Miscanthus sinensis × sinensis*] and GRC 14 [*M. sacchariflorus × sinensis*]; GRC 15, a novel *M. sacchariflorus × sinensis* clone; and GRC 9, a standard *Miscanthus × giganteus* clone) in Italy, Croatia, Germany and the UK. Over all trial locations and hybrids, the average aboveground biomass of the 3-year-old stands in August 2020 was $15 \, t \, DM \, ha^{-1}$ with nutrient contents of $7.6 \, mg \, N \, g^{-1}$ and $14.6 \, mg \, K \, g^{-1}$. As expected, delaying the harvest until spring reduced overall yield and nutrient contents ($12 \, t \, DM \, ha^{-1}$, $3.3 \, mg \, N \, g^{-1}$, and $5.5 \, mg \, K \, g^{-1}$). At lower latitudes, the late-ripening *M. sacchariflorus × sinensis* GRC 14 and GRC 15 combined high yields with low nutrient contents. At the most elevated latitude location (UK), the early-ripening *M. sinensis × sinensis* combined high biomass yields with low nutrient offtakes. The clonal *Miscanthus × giganteus* with intermediate flowering and senescence attained similar low nutrient contents by spring harvest at all four locations. Seasonal changes in yield and nutrient levels analysed in this study provide: (1) a first step towards recommending hybrids for specific locations and end uses in Europe; (2) crucial data for determination of harvest time and practical steps in the valorization of biomass; and (3) key sustainability data for life cycle assessments. Identification of trade-offs resulting from genetic × environment × management interactions is critical for increasing sustainable biomass supply from miscanthus grown on marginal lands.

1 | INTRODUCTION

The transition to a bioeconomy requires more biomass from agriculture. To avoid conflicts with food production and ensure sustainability criteria are met, biomass needs to be sourced where it is complimentary with farming systems, thus generating a wide range of co-benefits. Miscanthus is a leading perennial biomass crop combining traits that confer high radiation-, nutrient-, and water-use efficiencies. Once successfully established, it can tolerate challenging climates and soils with a range of marginality factors such as drought, salinity, and heavy metal contamination (Chen et al., 2017; Ezaki et al., 2008; Lewandowski et al., 2016; Pidlisnyuk et al., 2014; Pogrzeba et al., 2017; Rusinowski et al., 2019). Its perennial nature combined with its C_4 photosynthesis pathway results in relatively low fertilization demands (Kiesel, Wagner, et al., 2017; Wagner et al., 2019; Wagner & Lewandowski, 2017). In addition, miscanthus provides shelter for a range of animals (mainly birds and mammals), particularly over the winter (Lask et al., 2020). Its nearly year-round soil cover reduces soil erosion and run-off (Ferrarini, Serra, et al., 2017), and its efficient and deep rooting system and low fertilization requirements minimize nitrate leaching risks (Ferrarini, Fornasier, et al., 2017). For these reasons, miscanthus can make an essential contribution to future sustainable European agriculture.

This paper explores one major aspect of sustainability: nutrient offtake in the harvested biomass. There are important interactions between a hybrid's genetic composition (G), the location-specific environment (E), and management (M). Harvest approach and timing are critical for sustainability criteria [e.g. cutting height (Magenau et al., 2021)]. The miscanthus production cycle (for established *Miscanthus × giganteus* [*M × g*], *M. sacchariflorus × sinensis* [*M sac × sin*], and *M. sinensis × sinensis* [*M sin × sin*] in Europe) starts with shoots emerging from overwintering rhizomes in spring (mid-February to mid-May, depending on latitude). The shoots reach peak nutrient contents shortly after emergence as the plants draw nutrients from the rhizome and soil. As the aboveground biomass increases, the nutrient content starts to decrease, but the total nutrient stock in the aboveground biomass continues to rise. Generally, yield plateaus in late summer or early autumn, thought to be triggered by shortening photoperiods and declining temperatures. This coincides with carbohydrate and nutrient remobilization to the rhizomes used to power regrowth the following spring. In continental climates such as southern Germany, the standard clone *M × g* halves its nutrient contents by late October. It has been found that green biomass harvests (in particular for biogas) are possible without significant yield deficits the following years (Kiesel, 2020; Kiesel & Lewandowski, 2017; Mangold et al., 2019; Yates et al., 2015). If the harvest is delayed until the next spring (February or March), nutrient-use efficiencies are further increased (Cadoux et al., 2012; Cristian et al., 2006; Lewandowski et al., 2018; Mitros et al., 2020; Strullu et al., 2011).

This paper expands on earlier studies on the seasonal dynamics of nutrient contents in miscanthus (Beale & Long, 1997; Gołąb-Bogacz et al., 2021; Heaton et al., 2009; Himken et al., 1997; Jensen et al., 2017; Mos et al., 2021; Nassi o Di Nasso et al., 2011; Smith & Slater, 2011) by (1) including very diverse, novel, recently bred miscanthus hybrids; (2) extending the geographical distribution of test locations in Europe; and (3) increasing the temporal resolution of standing crop yield and nutrient contents. Key to this study are the common protocols used throughout growth and ripening to identify G × E factors influencing nutrient relocation to (during growth) and from (during senescence) the shoots and their impacts on yield, quality, and sustainability. Here we distinguish between physiologically active senescence and passive senescence caused by air frosts. Active senescence is controlled via complex regulatory pathways (Buchanan-Wollaston et al., 2003; Lim et al., 2007; Thomas & Stoddart, 1980). Both active and passive senescence are important in the pre-harvest ripening process (Clifton-Brown et al., 2001; Iqbal & Lewandowski, 2014; Jensen et al., 2017; Nassi o Di Nasso et al., 2011; Strullu et al., 2011), but their individual contributions and interactions remain unclear. In addition to internal translocation from shoot to rhizome over winter, nutrients are also relocated to the soil by leaf-fall and leaching of water-soluble nutrients following air frosts (Eichert & Fernández, 2012; Iqbal & Lewandowski, 2014).

By analysing seasonal changes in yield and nutrient levels of miscanthus, this study provides (1) a first step towards recommending specific hybrids for specific locations and end uses in Europe; (2) crucial data for determination of harvest time and practical steps in the downstream use of biomass (valorization); and (3) key data

for sustainability criteria using life cycle assessment methods. Identification of trade-offs resulting from G×E×M interactions is critical for increasing sustainable biomass supply from miscanthus grown on marginal lands.

2 | MATERIALS AND METHODS

2.1 | Field sites

The four trial sites are located:

- at Trawsgoed (TWS) near Aberystwyth, UK (52°24′59.8″N, 4°04′02.6″W);
- at Oberer Lindenhof (OLI) near Stuttgart, Germany (48°28′42.1″N, 9°18′41.0″E);
- near Zagreb (ZAG), Croatia (45°85′05.55″N, 16°17′77.7″E); and
- near Piacenza (PAC), Italy (45°00′34.9″N, 9°70′97.4″E).

The trial sites in TWS and PAC have a low altitude (72 and 73 m asl, respectively), ZAG is slightly higher (117 m asl), and OLI (706 m asl) has by far the highest altitude.

At all four sites, a time-zero soil coring was conducted in autumn 2017 to characterize the soil profile and quantify soil nutrients (Table 1). Field trials were planted with 14 miscanthus seed- or rhizome-based hybrids in spring 2018 in a randomized complete block design with four replicates. This study analyses four of these 14 hybrids (Figure 1): GRC 3 (*Miscanthus sinensis × sinensis* [*M sin × sin*]) and GRC 14 *(M. sacchariflorus × sinensis* [*M sac × sin*]), two novel seed-based hybrids; GRC 15, a novel rhizome-based clone (*M sac × sin*); and GRC 9, a standard rhizome-based clone of *M. × giganteus* (*M × g*). At three plants m^{-2}, GRC 3 was planted at double the planting density of the other three hybrids (1.5 plants m^{-2}). The TWS field trial was planted on an improved, high-input grassland field used for silage production and grazing. At OLI, the field was fertilized regularly with horse manure in the years before the miscanthus trial was planted. This slow-release nutrient source could have limited nutrient availability during miscanthus establishment, but it is unlikely. At ZAG, miscanthus was planted on a marginal field with heavy clay soil prone to both drought and waterlogging. Here, poor soil-to-plant hydraulic contact and poor weed control during establishment resulted in high seedling mortality rates, and surviving plants were replanted at the target densities in spring 2019. At PAC, the soil and climate conditions in 2018 were highly conducive to establishment, achieving >95%, and no replanting was required in 2019. After planting, no fertilizers were applied to any of the sites. Further trial details are described in Awty-Carrol et al. (2022).

TABLE 1 Average values of crucial soil parameters at 0–30 cm depth for each field site in autumn 2017

	Soil texture	pH	Soil organic carbon (%)	Total nitrogen (%)	Plant-available phosphate (P$_2$O$_5$; mg kg^{-1})	Plant-available potassium (K$_2$O; mg kg^{-1})	Total calcium (mg kg^{-1})	Total magnesium (mg kg^{-1})
TWS	Sandy loam	5.9	2.26	0.42	63.3	288.3	1869.8	6253.3
OLI	Clay loam	6.9	1.41	0.24	229.9	520.1	4672.3	4615.0
ZAG	Silt loam	5.2	1.07	0.18	384.5	309.0	3140.0	5077.5
PAC	Clay loam	8.2	0.64	0.19	134.8	510.1	3803.0	10034.0

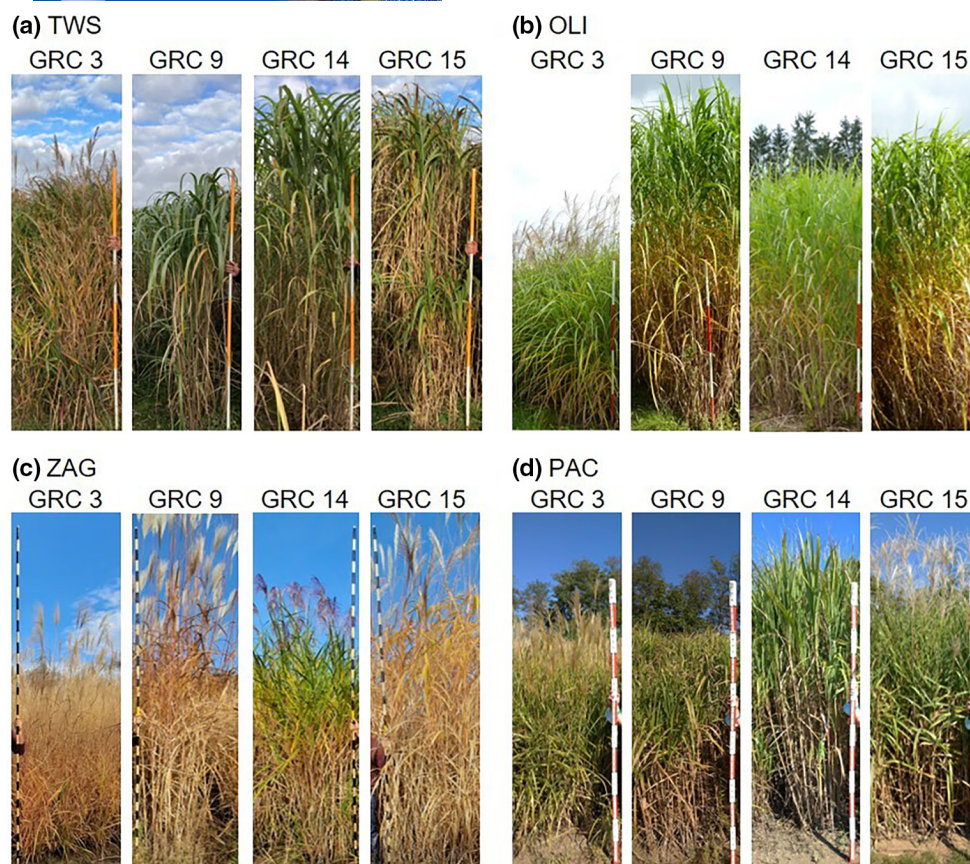*Note:* TWS: Trawsgoed, UK; OLI: Oberer Lindenhof, Germany; ZAG: Zagreb, Croatia and PAC: Piacenza, Italy.

FIGURE 1 Images of the two novel seed-based miscanthus hybrids GRC 3 (*Miscanthus sinensis × sinensis*) and GRC 14 (*M. sacchariflorus × sinensis*); GRC 15, a novel clone (*M. sacchariflorus × sinensis*); and GRC 9, a standard clone of *M. × giganteus* at the four trial sites ((a) TWS: Trawsgoed, UK; (b) OLI: Oberer Lindenhof, Germany; (c) ZAG: Zagreb, Croatia and (d) PAC: Piacenza, Italy) in October 2020. Height of measuring stick: TWS and OLI 2 m, ZAG 3.4 m and PAC 3 m.

Between January 2020 and March 2021, air temperatures and precipitation were recorded at each field trial at hourly intervals 2 m above the soil surface using a WS-GP 1 weather station (Delta-T Devices Ltd). Long-term daily temperature and monthly total precipitation from 2012 to 2019 were obtained from the nearest weather station.

2.2 | Field measurements

Standing crop yields were estimated using a shoot subsampling approach devised in an earlier project (Nunn et al., 2017). This approach involves harvesting 10 randomly selected shoots per plot throughout the growing season (serial cut) and relating the weight of this shoot subsample at final harvest in spring (February or March) to the yield determined by a harvest area (black rectangle in Figure 2). The serial cut was taken from outside the harvest area but within the plot to minimize border effects and avoid compromising the final harvest area yield through the removal of shoots. The random selection of the 10 shoots of the serial cut was ensured by inserting a

pre-marked stick through one of the sampling rows next to the harvest area (Figure 2). Two shoots from each of five plants in the row, which were nearest the marks and fulfilled the criteria of contributing to the canopy and therefore the yield (defined as shoots with a height at least 60% of canopy height), were cut at 10 cm. Sampling rows around the harvest area were advanced in a clockwise direction at each sampling date (Table 3). This approach minimizes sampling damage and helps maintain the integrity of the canopy. Harvested shoots were separated into leaf and stem fractions by removing the leaves at the ligule. Each leaf fraction was divided into green and brown leaves. For each location and hybrid, standing crop yields were estimated separately at monthly intervals using Equation (1):

$$\text{yield}_n = \frac{\text{ten shoots}_n}{\text{ten shoots}_s} \times \text{yield}_s \tag{1}$$

where yield_n is the dry matter (DM) yield on sampling date n (t DM ha^{-1}), yield_s is the DM yield of the harvest area at spring harvest (t DM ha^{-1}), ten shoots_n is the total weight
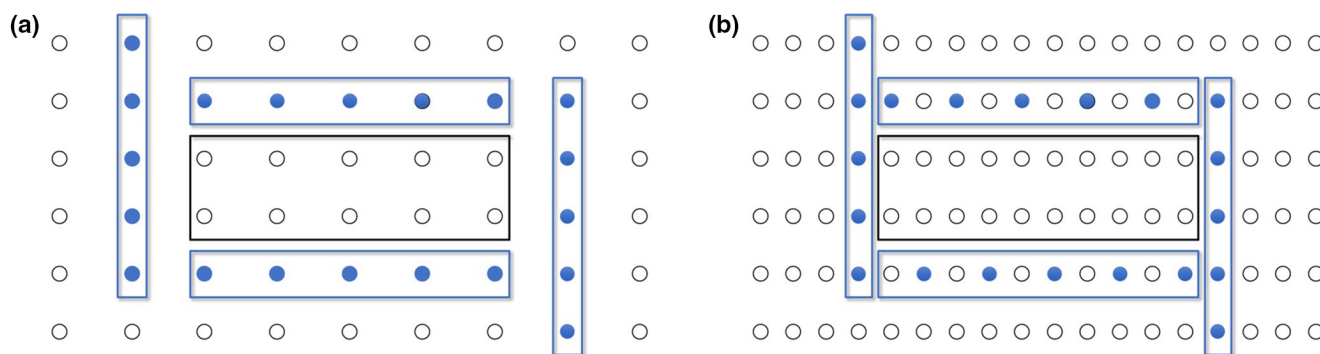
FIGURE 2 Sampling areas within the plots with (a) lower planting density of 1.5 plants m^{-2} (GRC 9, 14, and 15) and (b) higher planting density of 3 plants m^{-2} (GRC 3). The harvest area (black rectangle) was harvested in spring. From May until spring harvest, samples were taken from plants in the rows next to the harvest area (blue rectangles). Two shoots were taken from each sampled plant (blue circles). At each sampling date, the next row (blue rectangle) was sampled, moving in a clockwise direction. (GRC 3 [*Miscanthus sinensis × sinensis*] and GRC 14 [*M. sacchariflorus × sinensis*], two novel seed-based miscanthus hybrids; GRC 15, a novel clone [*M. sacchariflorus × sinensis*]; and GRC 9, a standard clone of *M. × giganteus*).

TABLE 2 Characterization of the miscanthus hybrids according to flowering and greenness into ripening classes

Hybrid	GRC 3	GRC 9	GRC 14	GRC 15
	Miscanthus sinensis × sinensis (*M sin × sin*)	*Miscanthus × giganteus* (*M × g*)	*Miscanthus sacchariflorus × sinensis* (*M sac × sin*)	*Miscanthus sacchariflorus × sinensis* (*M sac × sin*)
	Seed-based	Rhizome-based	Seed-based	Rhizome-based
Flowering	Early	Medium	Late	Medium
Greenness	Late	Medium	Late	Early
Ripening	Early	Medium	Late	Medium

of the 10 stems on sampling date n (g) and ten shoots$_s$ is the total weight of the 10 stems at spring harvest (g).

At some sites, when winter snowfall lodged and buried the crop, the regular monthly shoot samples could not be taken until the snow had cleared (see Table 3 for sampling dates). Flowering stages (on a 0–5 scale) were recorded fortnightly for five plants within the harvest area of each plot (Figure 2). Flowering initiation was defined as the appearance of the flag leaf (stage 1), which is shortly followed by panicle emergence (stage 2), and anthesis (stage 3). Dates when plants reached flowering stage 1 were used to classify the hybrids into three flowering categories (early, medium, and late). Additionally, the hybrids were divided into three greenness categories according to visual greenness scores in autumn 2020 (Figure 1). The greenness categories were defined as: early = hybrid with the lowest; medium = hybrids with a medium; and late = hybrid with the highest proportion of green leaves. Pursuant to the flowering and greenness categorization, the four hybrids were classified into three ripening classes (Table 2). The lodging of the hybrids was rated per plot using a score

between 0 (all plants standing perfectly erect and showing no signs of lodging) and 9 (plants in the entire plot lying flat on the ground). Severe lodging was thus characterized by a score above 5.

2.3 | Laboratory analysis

To determine the DM content, the biomass of stem, green leaf, and brown leaf from the 10 shoot samples per plot was dried to constant weight at 80°C in a drying cabinet. The samples listed in Table 3 were analysed for ash and nutrient contents.

Each separated and dried plot-level sample was milled (SM 200; Retsch, Haan fitted with a 1 mm sieve). Ash and mineral content were determined according to VDLUFA Method Book III (Naumann & Bassler, 1976). For ash content, the samples were incinerated in a muffle kiln at 550°C for 4 h. For P, K, Ca, and Mg contents, 0.5 g of each sample was diluted with 8 ml HNO$_3$ (concentration 65%) and 6 ml H$_2$O$_2$ (concentration 30%) and digested in an

TABLE 3 Sample analysis schedule for ash and nutrient contents

Year	Calendar week	Location	Analysed samples
2020	19	PAC	Total shoot
	21	All	
	25	All	
	29	All	
	33	All	
	35	All	
	37	All	
	39	All	
	41	All	
	43	All	
	45	PAC	Leaves and stems separately
	47	TWS, OLI, ZAG	
	49	PAC	
	51	All	
2021	2	TWS, OLI, ZAG	
	5	PAC	
	6	TWS, OLI, ZAG	
	10	TWS, OLI	

Note: TWS: Trawsgoed, UK; OLI: Oberer Lindenhof, Germany; ZAG: Zagreb, Croatia and PAC: Piacenza, Italy.

ETHOS lab microwave (MLS GmbH). The extracts of the digested samples were analysed using an ICP-OES at the Core Facility Hohenheim. The N content was determined according to the Dumas principle using a Vario Macro Cube (Elementar Analysensysteme GmbH).

For each location and hybrid, the nutrient stocks in the aboveground (above 10 cm) standing crop were calculated separately according to Equation (2):

$$\text{nutrient stock}_n = \text{nutrient content}_n \times \text{yield}_n \quad (2)$$

where $\text{nutrient content}_n$ is the nutrient content on sampling date n (kg [t DM]$^{-1}$) and yield_n is the biomass yield on sampling date n (t DM ha^{-1}).

For each location and hybrid, the passive nutrient translocation rate was calculated according to Equation (3):

$$\text{passive translocation rate} = \frac{(\text{yield}_p - \text{yield}_s) \times \text{nutrient content}_s}{\text{nutrient stock}_p - \text{nutrient stock}_s} \quad (3)$$

where yield_p is peak DM yield (t DM ha^{-1}), yield_s is DM yield at spring harvest (t DM ha^{-1}), $\text{nutrient content}_s$ is nutrient content at spring harvest (kg [t DM]$^{-1}$), nutrient stock_p is nutrient stock at peak yield (kg ha^{-1}) and nutrient stock_s is nutrient stock at spring harvest (kg ha^{-1}).

2.4 | Statistical analysis

The data were statistically analysed using a linear model (Eisenhart, 1947). The model can be described as:

$$y_{ijlk} = \mu + g_i + s_j + (gs)_{ij} + (st)_{jl} + (gt)_{il} + (rs)_{jk} + (rst)_{jkl} + (gst)_{ijl} + e_{ijlk}$$

where μ is the intercept; g_i is the ith hybrid effect; s_j is the jth site effect; t_l is the lth time of sampling effect; $(gt)_{il}$ is the interaction effect of the ith hybrid with the lth time of sampling effect; $(sr)_{jk}$ is the effect of the kth field replicate in the jth site; $(rst)_{jkl}$ is the fixed effect of the kth field replicate in the jth site at the lth time of measurement effect; $(gst)_{ijl}$ is the interaction effect of the ith hybrid effect with the jth site at the lth time of sampling effect; and e_{ijlk} is the residual error term corresponding to y_{ijlk}. All effects except the error were assumed to be fixed. For the error effects of the same plot, site-specific first-order autocorrelation with time of measurement-specific variance was fitted. Thus, the model enables the estimation of time-of-measurement-specific variances and a correlation of error effects of the same plot across measurements times for each site. Where significant differences measured via global F test were found, a Fishers LSD test was performed for multiple comparisons. A letter display was used to present

—WILEY | **1041**

results of multiple comparisons. The weighted least-square means were estimated and are presented with their standard deviation or a corresponding letter display in the results section. Pre-requirements of homogeneous variance and normal distribution of residuals (despite the heterogeneity already accounted for by the model) were checked graphically using residual plots. In cases of deviations from the assumptions, the data were square-root or logarithmically transformed. In such cases, means were back-transformed. Standard deviations were back-transformed using the delta method.

At the beginning of the growing season, the quantities of biomass collected from the 10 shoots of the serial-cut samples were insufficient for separate chemical analysis of the four replicates at TWS and OLI. A bulked sample per genotype was analysed. Results were plotted in the time courses but were excluded from the statistical analysis.

The statistical analysis was performed using the PROC MIXED procedure of Statistical Analysis Software SAS version 9.4 (SAS Institute, Inc.). Figures were produced with the package ggplot2 (Wickham, 2009) of the R program (R Core Team, 2019).

3 | RESULTS

3.1 | Environmental conditions

Figure 3 shows the average daily temperature, total monthly precipitation from April 2020 to March 2021, and the eight-year average data for each location from 2012 to 2019. In 2020, the warmest trial site was PAC (average yearly temperature 13.9°C), followed by ZAG (11.7°C) and TWS (10.7°C). OLI (8.7°C) was the coldest location due to its higher altitude. Compared to the 8-year average temperature, the growing season in 2020–2021 was slightly colder than average at ZAG, within the average range at TWS and OLI, but considerably colder than average at PAC.

Air frosts occurred at each location during the winter. However, the dates of the first frosts in autumn and the lowest daily average air temperature differed substantially
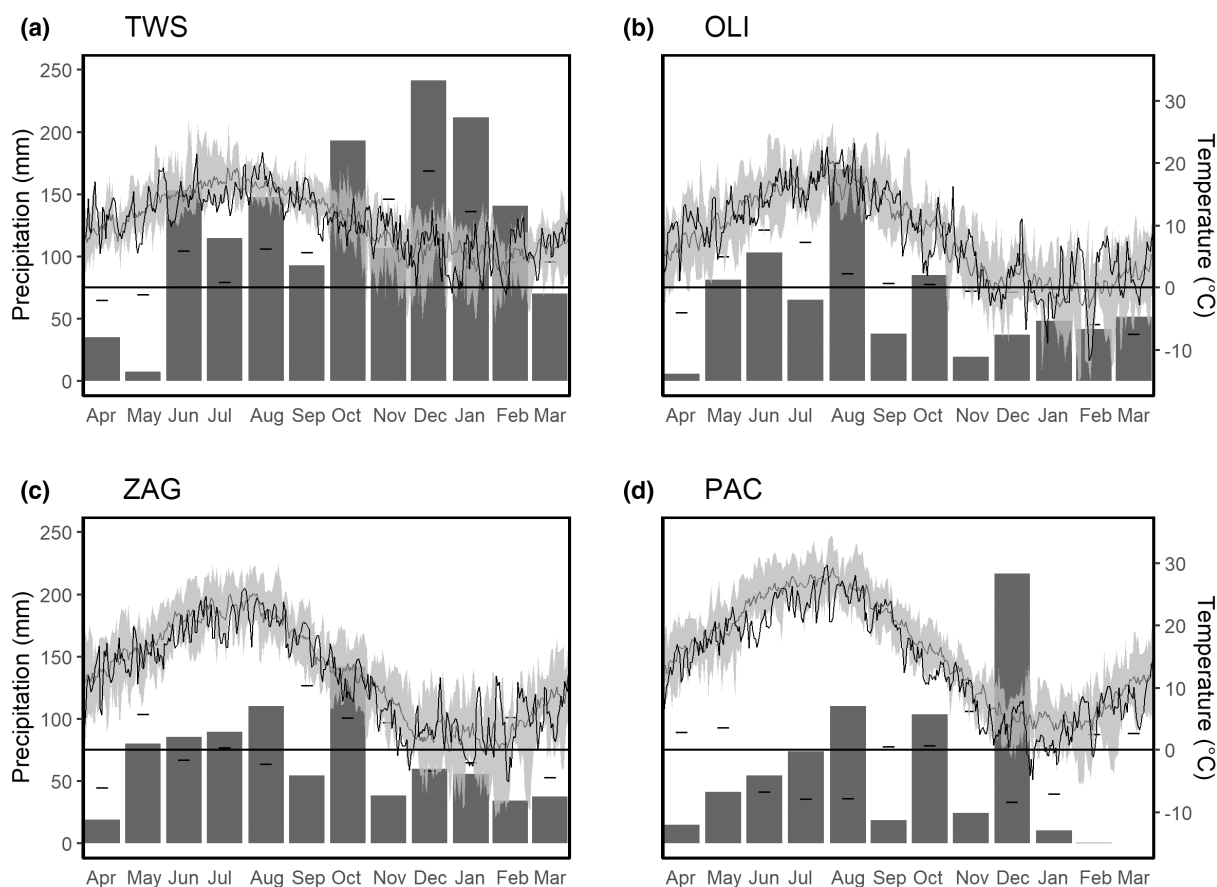

FIGURE 3 Average daily air temperature (2 m above soil surface; black line) and cumulative monthly precipitation (bars) from April 2020 to March 2021, eight-year daily average temperature (from 2012 to 2019, grey line), eight-year daily minimum and maximum temperature (grey area), and eight-year average precipitation (dashes) at the four trial sites: (a) TWS: Trawsgoed, UK; (b) OLI: Oberer Lindenhof, Germany; (c) ZAG: Zagreb, Croatia; and (d) PAC: Piacenza, Italy (horizontal line: 0°C).

between sites. By far the lowest average daily temperature (calculated from hourly values) was recorded at OLI (−11°C), followed by ZAG (−5.1°C), PAC (−4.8°C), and TWS (−1.1°C). At OLI, the first frost occurred at the beginning of October 2020, whereas at ZAG and PAC, the temperature dropped below 0°C for the first time in mid-November and at the end of November 2020, respectively. The most extended frost-free period was recorded at TWS, where the first frost occurred at the beginning of December.

The highest total precipitation in 2020 was recorded at TWS (1484 mm). The total precipitation ranged between 740 and 801 mm at the other three sites—relatively low values compared with previous years. The beginning of the growing season was dry at all four sites. However, rainfall in June and July together with the available ground water was sufficient to prevent soil water deficits exceeding the soil plant-available water and maintain growth rates over the summer. September and November were unseasonably dry, especially at PAC, but high rainfall in December at PAC resulted in excess water. Heavy snowfalls at OLI and PAC in December lodged the miscanthus crop, affecting the biomass yield (Figure 4) and the leaf-to-stem ratio at spring harvest (Figure 5). This heavy snowfall is unusual for PAC.

3.2 | Biomass yield and leaf-to-stem ratio

Figure 4 shows the monthly average aboveground DM yield per hybrid and location from May 2020 until spring
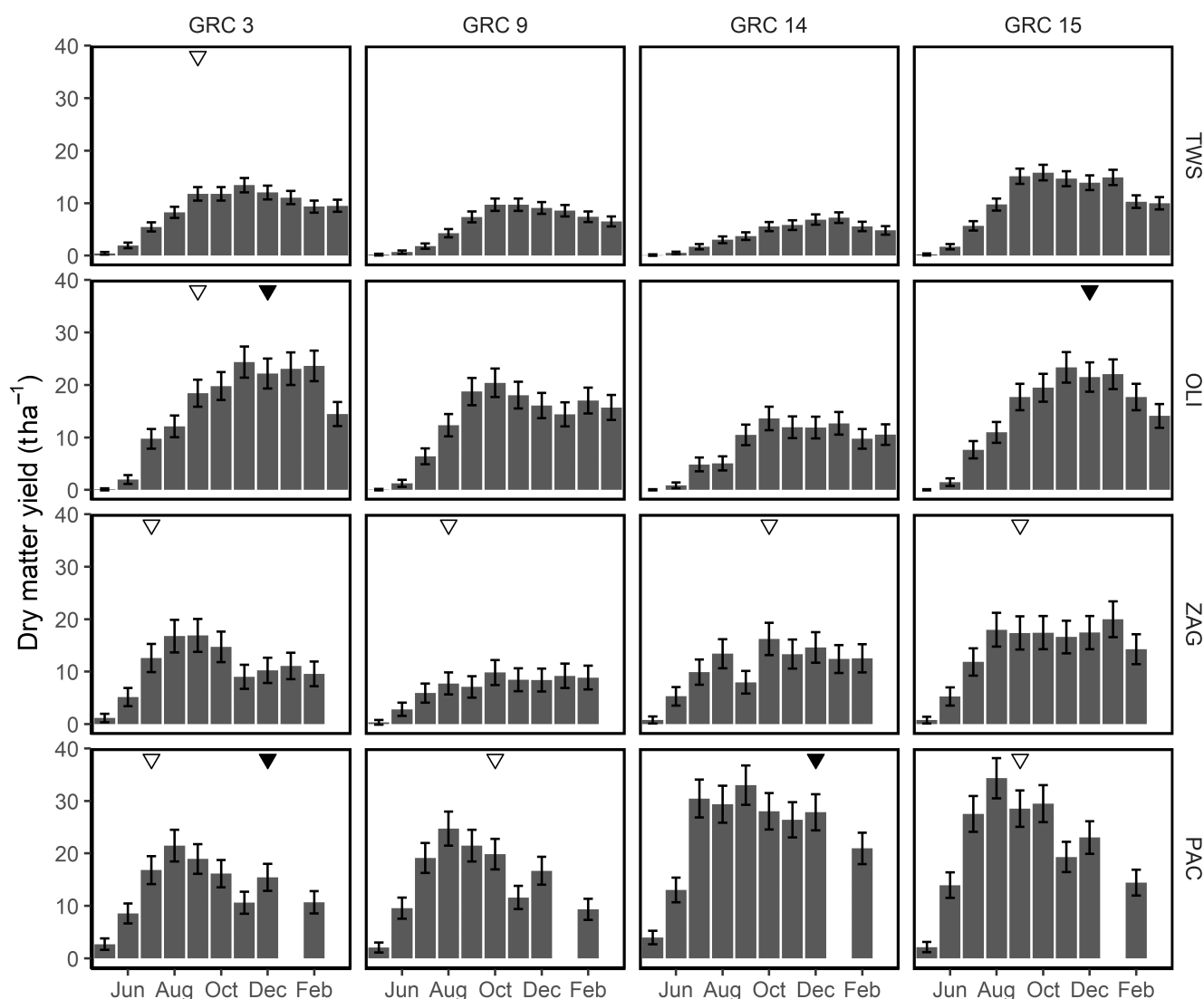

FIGURE 4 Monthly average aboveground dry matter yield of two novel seed-based miscanthus hybrids, GRC 3 (*Miscanthus sinensis × sinensis*) and GRC 14 (*M. sacchariflorus × sinensis*); GRC 15, a novel clone (*M. sacchariflorus × sinensis*); and GRC 9, a standard clone of *M. × giganteus* at four locations (TWS: Trawsgoed, UK; OLI: Oberer Lindenhof, Germany; ZAG: Zagreb, Croatia, and PAC: Piacenza, Italy). Error bars indicate standard deviations, ▽ the onset of flowering, and ▼ the beginning of severe lodging.
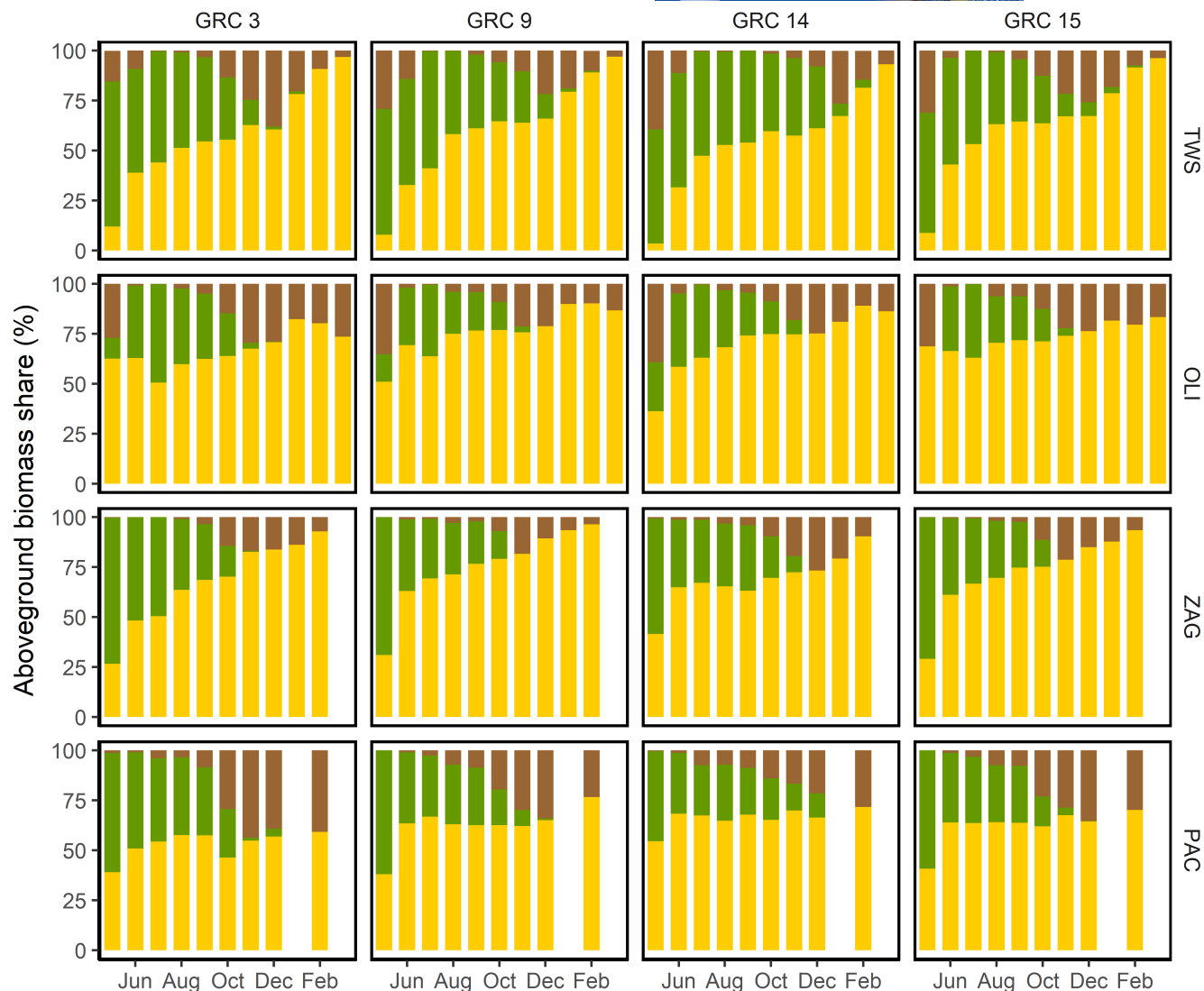
FIGURE 5 Average monthly brown leaf (brown), green leaf (green), and stem (yellow) share of the estimated aboveground biomass yield per month for two novel seed-based miscanthus hybrids, GRC 3 (*Miscanthus sinensis × sinensis*) and GRC 14 (*M. sacchariflorus × sinensis*); GRC 15, a novel clone (*M. sacchariflorus × sinensis*); and GRC 9, a standard clone of *M. × giganteus* at four locations (TWS: Trawsgoed, UK; OLI: Oberer Lindenhof, Germany; ZAG: Zagreb, Croatia and PAC: Piacenza, Italy).

harvest in 2021, and also the onset of flowering and severe lodging. Across all hybrids, the highest average yield at spring harvest was achieved at OLI and PAC (14 t DM ha⁻¹), followed by ZAG (11 t DM ha⁻¹) and TWS (8 t DM ha⁻¹). At the warmer lower-latitude sites, peak yield was generally achieved by late August (PAC) or September (ZAG), but not until a month later at OLI and TWS. After the peak in late summer/autumn, yield declines were most substantial at PAC (−52%), followed by TWS (−33%), OLI (−31%), and ZAG (−26%). At OLI and PAC, biomass losses were affected by severe lodging from December onwards due to snow. Lodging impacted the yield assessment by breaking off stems but at the same time prevented leaf-fall, which resulted in higher leaf proportions at the two locations (Figure 5). At both locations, the hybrid most affected by lodging was GRC 3. At PAC, GRC 3 and 14 lodged and

were covered by a layer of snow and ice, while GRC 9 and 15 stood well until spring harvest, only losing shoot tips. In contrast, at OLI, GRC 3 and 15 lodged severely and were covered by a snow and ice layer almost the entire winter. This severe lodging led to nearly twice the amount of biomass lost (41%) before harvest compared to the less affected hybrids GRC 9 and 14 (23%). At PAC however, the severely lodged hybrids GRC 3 and 14 had lower monthly biomass losses (43%) than the non-lodging hybrids (60%). The *M sin × sin* hybrid GRC 3 was the only hybrid to reach flowering at all four locations and, unlike the other hybrids, reached peak yield after flowering. At the southerly latitudes of ZAG, flowering initiation was observed in all four hybrids, but at PAC, GRC 14 did not reach flowering.

Figure 5 shows the development of the green and brown leaf-to-stem proportion throughout the season. In

general, the stem share increased from spring emergence until harvest the following spring, with a period of a relatively stable leaf-to-stem ratio from late summer until autumn. At the beginning of the growing season, the harvested biomass mainly consisted of green leaves above the cutting height of 10 cm. However, at TWS and OLI, late spring frosts damaged emerging shoots, which can be seen in the early season brown leaf fractions. From July onwards, brown leaf fractions increased at OLI, PAC and ZAG, and from mid-August at TWS. In contrast to brown leaf fractions caused by frost damage which impacts the top leaves, these indicators of senescence in mid- to late summer occur below the leaf canopy after canopy closure starves lower leaves of light. The maximum proportion of brown leaves in the aboveground biomass was observed in autumn or winter and decreased afterwards due to leaf-fall.

Location and genetics affected the senescence of the hybrids in autumn. No green leaves were found at the ZAG site at the end of October, except for GRC 14. Some green leaves were still found at the OLI site in October, but none in November. At both locations, frosts with temperatures below −5°C occurred in November, which may have caused leaves to die. By contrast, green leaves were still found in December at PAC (GRC 14) and even shortly before harvest in March at TWS, even though (mild) frost events were recorded over winter at both locations. At TWS, GRC 3 senesced first, the only flowering hybrid at that location. Of the four hybrids, GRC 14 stayed green the longest, resulting in the highest moisture contents at harvest (Awty-Carrol et al., 2022). At OLI and PAC, all hybrids still had high leaf shares at harvest due to lodging. The leaf share at OLI decreased slightly over winter, as sampling was affected by snow and ice covering the lodging crop.

3.3 | Ash and nutrient content

Figure 6 shows the development of ash and nutrient content from May until spring the following year. In general, ash and nutrient contents decreased from the beginning of the vegetation period until spring harvest. At the beginning of the vegetation period, the highest values of the four locations were found at TWS and OLI, which may be related to later emergence and slower growth due to colder temperatures in spring. Contents of ash, nitrogen (N), and phosphorus (P) decreased until August, and then remained relatively stable until harvest in the following spring. The potassium (K) content also decreased sharply until August, but this was followed by a slow decrease until October and then a relatively stable content level until harvest in March. In

general, the ash content was more than halved from the beginning of the vegetation period to mid-October and declined in total by 67%. At the same time, the N content decreased on average by 87% (ZAG 94%, OLI 90%, PAC 88%, and TWS 74%), P by 79% and K by 82% (ZAG 98%, PAC 87%, OLI 84%, and TWS 70%). For calcium (Ca) and magnesium (Mg), the decline from emergence to harvest was not as distinct as for the other minerals analysed. The highest Mg contents were found at TWS, the only trial established on former grassland, and may have been impacted by the short vegetation period at this most northern site. However, GRC 3, the only flowering hybrid at that site, reached the same level as the other locations at spring harvest.

GRC 14 had the significantly highest N, P, and K contents and GRC 3 the lowest. While GRC 3 (early-ripening) showed signs of senescence in autumn, GRC 14 (late-ripening) had the latest flowering times of all the hybrids and stayed green at all locations until frosts killed the aboveground biomass. From July onwards, the significantly highest N content and from the end of October onwards the highest K content was found at TWS for each hybrid. At harvest, the N content at TWS (average 7.6 g mg^{-1}) was four times higher than at the other locations.

Over winter, the decrease in ash and N content was mainly due to leaf-fall, as the levels in stems (except ash in GRC 14 at TWS) and leaves remain relatively constant (Figure 7). It is noteworthy that even at TWS, where no severe frosts occurred, an internal translocation was observed, indicated by decreased content within the aboveground biomass. In addition to ash, an active translocation over winter was also observed for K and Mg in leaves and stems and for N, P, and Ca in leaves. However, locations with autumn frosts had relatively stable nutrient contents in stems and leaves over winter. The results show that mild winter temperatures can be beneficial for the reduction of ash and nutrient contents. However, this could not entirely compensate for the slower, incomplete crop development of late-ripening hybrids (e.g. GRC 14 at TWS) caused by lower temperatures during the vegetation period, thus leading to higher N, K, and Mg contents at harvest.

3.4 | Nutrient stock

Figure 8 shows the development of total N, P, K, Ca, and Mg stock accumulated in the aboveground biomass during the vegetation period until final harvest in spring 2021. It is equivalent to the nutrient offtake which would be removed by the biomass if harvested at this time. Generally, the nutrient stock increased with biomass accumulation during the vegetation period and reached
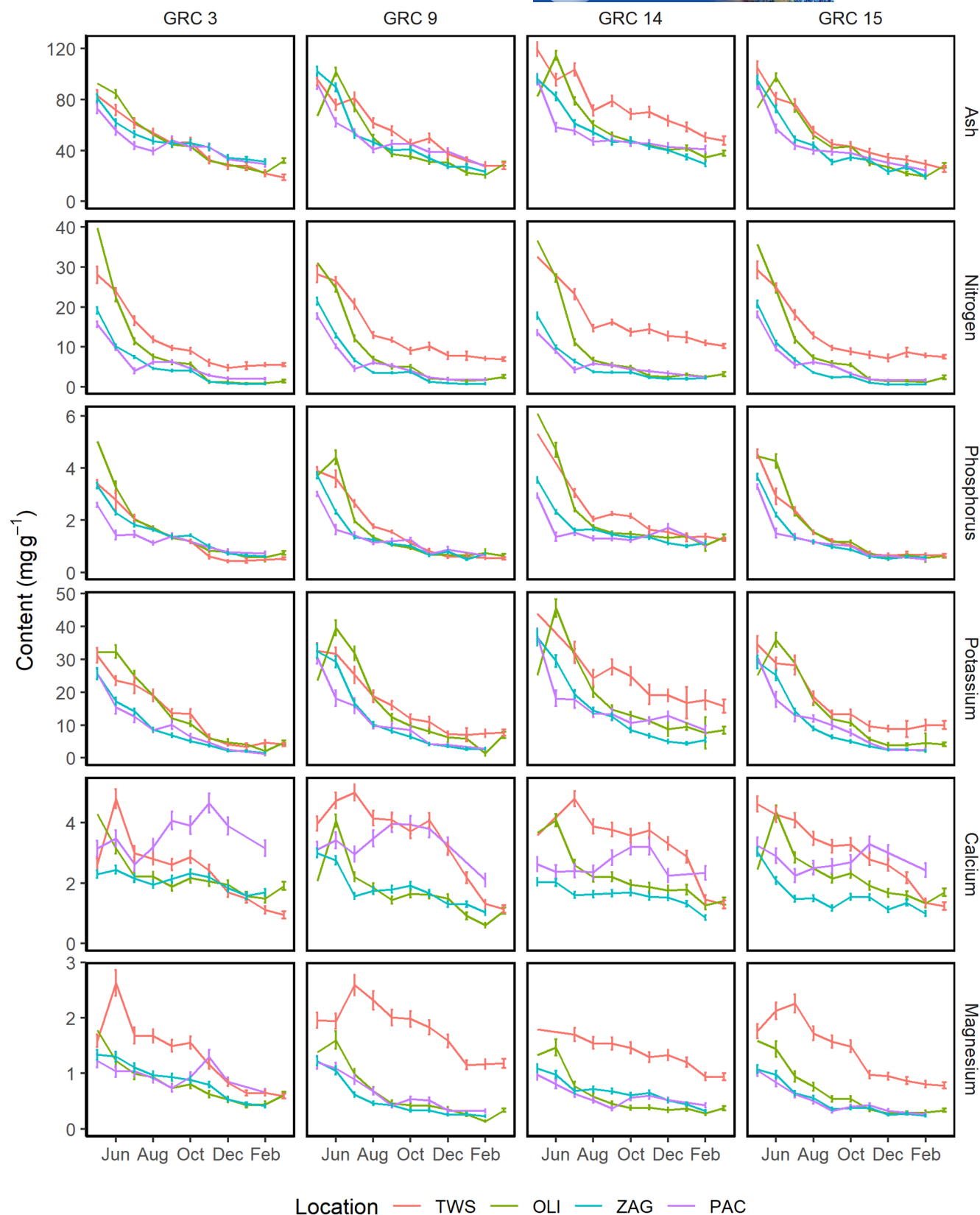
FIGURE 6 Mean ash, nitrogen, phosphorus, potassium, calcium, and magnesium content in $mg\,g^{-1}$. Error bars indicate standard deviations ($n = 4$, except for August to October when $n = 8$, OLI in May $n = 1$ and TWS GRC 14 in May $n = 2$, due to shortage of material; GRC 3 [*Miscanthus sinensis × sinensis*] and GRC 14 [*M. sacchariflorus × sinensis*], two novel seed-based miscanthus hybrids; GRC 15, a novel clone [*M. sacchariflorus × sinensis*]; and GRC 9, a standard clone of *M. × giganteus*; TWS: Trawsgoed, UK; OLI: Oberer Lindenhof, Germany; ZAG: Zagreb, Croatia, and PAC: Piacenza, Italy).
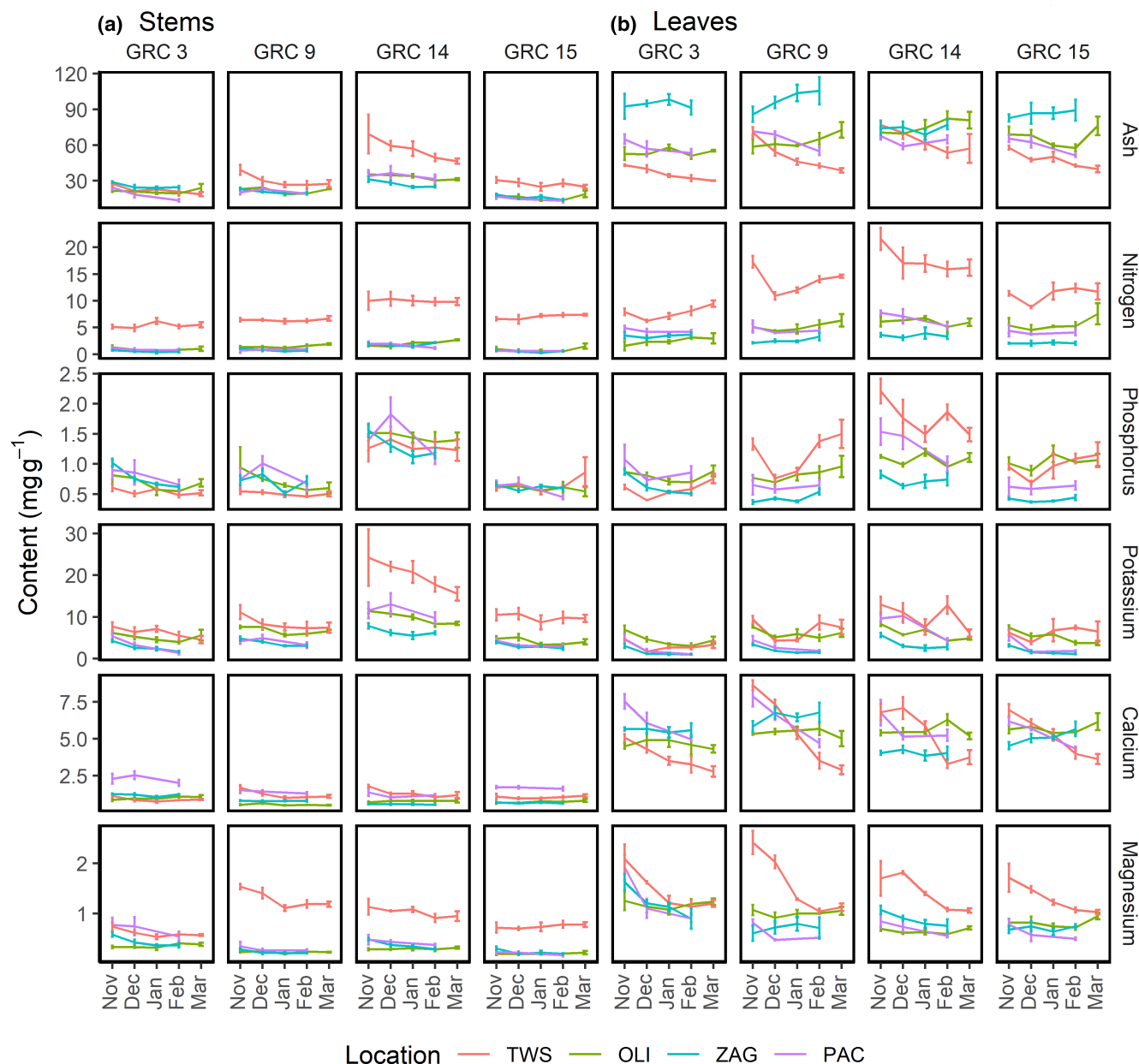
FIGURE 7 Mean contents of ash, nitrogen, phosphorus, potassium, calcium, and magnesium in mg g^{-1} in (a) stems and (b) leaves per hybrid and location. Error bars indicate standard deviation ($n = 4$; GRC 3 [*Miscanthus sinensis × sinensis*] and GRC 14 [*M. sacchariflorus × sinensis*], two novel seed-based miscanthus hybrids; GRC 15, a novel clone [*M. sacchariflorus × sinensis*]; and GRC 9, a standard clone of *M. × giganteus*; TWS: Trawsgoed, UK; OLI: Oberer Lindenhof, Germany; ZAG: Zagreb, Croatia, and PAC: Piacenza, Italy).

a peak in summer. For this reason, the highest nutrient stocks were often observed for the PAC site due to its high biomass productivity (Figure 4). Of the nutrients considered, K and N had the overall highest nutrient stocks (up to 488 kg K ha^{-1} and 213 kg N ha^{-1}).

The highest N stock was recorded at PAC and the lowest at ZAG and correlated strongly with aboveground biomass formation. However, the highest nitrogen offtake at spring harvest was observed for the least productive site TWS (Appendix S1), showing that the vegetation period was too short for most hybrids at this site to finish their

growth cycle, and mild temperatures during winter only slightly promoted overwinter ripening. The second highest N offtakes at final harvest in spring were mostly found at OLI, followed by PAC and ZAG. The higher N offtakes at OLI and PAC are related to a higher aboveground biomass production, but may also have been affected by lodging, which reduced leaf-fall (Figure 5). The highest peak N stock (average over the four hybrids) was found at PAC (168 kg N ha^{-1}), followed by TWS (113 kg N ha^{-1}), OLI (98 kg N ha^{-1}), and ZAG (71 kg N ha^{-1}). The peak N stock was reached first at ZAG and PAC in July and August,
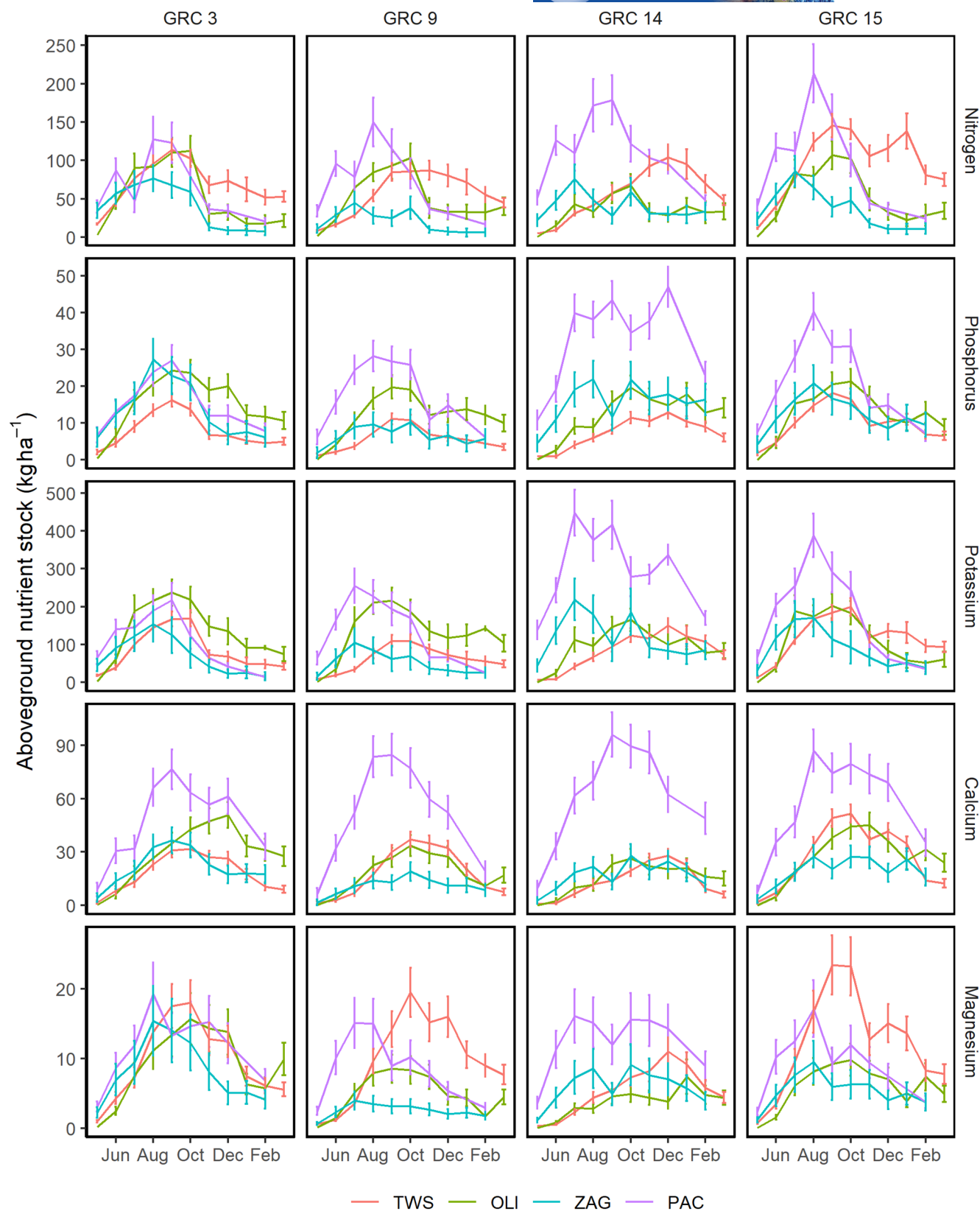
FIGURE 8 Nitrogen, phosphorus, potassium, calcium, and magnesium stocks in kg ha⁻¹ per hybrid and location. Error bars indicate standard deviations ($n = 4$, except for August to October where $n = 8$, OLI in May $n = 1$ and TWS GRC 14 in May $n = 2$ due to shortage of material; GRC 3 [*Miscanthus sinensis×sinensis*] and GRC 14 [*M. sacchariflorus×sinensis*], two novel seed-based miscanthus hybrids; GRC 15, a novel clone [*M. sacchariflorus×sinensis*]; and GRC 9, a standard clone of *M.×giganteus*; TWS: Trawsgoed, UK; OLI: Oberer Lindenhof, Germany; ZAG: Zagreb, Croatia, and PAC: Piacenza, Italy).

respectively, then at OLI, and finally at TWS in, or even after, September. The decrease in N stock (relocation rate) from peak nutrient stock until final harvest in spring was highest at PAC (84%), followed by ZAG (80%), OLI (65%), and TWS (51%). GRC 14 had the lowest relocation rate of the four hybrids, except at TWS. The amount of N nutrients lost by the leaf and stem biomass between peak N stock and harvest (passive relocation) can, in general, explain 55% of the N stock decrease (TWS 100%, OLI 54%, PAC 34%, and ZAG 22%).

The highest peak K stocks were recorded for GRC 14 and 15 at PAC, with all other hybrids and locations in a similar lower range. The highest K stock at spring harvest was found for GRC 14 at PAC (170 kg K ha^{-1}). The other three hybrids at this site had, on average, 85% lower offtakes, leading to an 18-percentage-point lower relocation rate of the late-ripening GRC 14 (63%). At ZAG, the offtake ranged between 16 kg K ha^{-1} (GRC 3) and 85 kg K ha^{-1} (GRC 14) with a relocation rate of 56%–90% (average 75%). At TWS, the offtakes of GRC 14 and 15 were double those of GRC 3 (42 kg K ha^{-1}). At OLI, no significant differences between the four hybrids were found (average 81 kg K ha^{-1}). The two sites with late-emerging hybrids, TWS and OLI, had the lowest relocations rates (average: 58% and 61%, respectively). For GRC 14, the hybrid with the lowest relocation rate at each location (average 55%), no significant difference in offtakes was found between the sites. For the other three hybrids by contrast, the K offtake was significantly higher at TWS than at PAC. Of all four hybrids, GRC 3 relocated K most efficiently (86%) at all three locations except OLI (78%).

4 | DISCUSSION

This study presents seasonal dynamics of aboveground scientifically harvested yield, nutrient contents and nutrient stocks for four novel miscanthus hybrids monitored in the third growing season at four widely distributed sites traversing a large part of the European climate. Nutrient contents and stocks showed that site (environmental) differences were more prominent than the differences between hybrids (genetic). Creating detailed information on the seasonal dynamics of aboveground yield and the nutrient fluxes and stocks of hybrids grown in different environments helps provide selection criteria for the most sustainable hybrids and their associated agronomies, which need to be matched to various biomass logistical and utilization chains. These dynamics play an important role in analysing the interactions between biomass yield and compositional qualities to determine optimal harvest windows, increase sustainability, and identify which hybrid types are best suited to each location.

4.1 | Yield and nutrient contents in spring after winter ripening

The highest spring yields after the third growing season were achieved by different hybrids at each location: in northern Europe, *M sin × sin* and the rhizome-based *M sac × sin*; in central Europe, *M sin × sin* and *M × g*; and in southern Europe, *M sac × sin*. This contrasts with the results of Kalinina et al. (2017), where one *M sin × sac* hybrid and the standard *M × g* produced the highest yields at all European sites. Aboveground yields of this study ranged, across all sites and hybrids, from 5 to 21 t DM ha^{-1}. Across all four hybrids, the lowest yields were recorded at the TWS site in the UK (8 t DM ha^{-1}), and the highest at OLI in southern Germany and PAC in northern Italy (both averaged 14 t DM ha^{-1}). The average spring yield achieved in Croatia (ZAG) was 11 t DM ha^{-1}, significantly lower than that at OLI and PAC but significantly higher than TWS. Those yields were obtained with the same scientific protocol. Actual biomass yields in conventional harvest systems are likely to be approximately 10.0%–14.4% lower due to a generally 10–15 cm higher stubble height (Magenau et al., 2021). Furthermore, harvest losses are higher due to swath drying prior to baling or wind blow of direct chipped biomass during filling of trailers.

For the standard *M × g*, the spring yields were relatively low at the UK (6.5 t DM ha^{-1}) and Croatian site (8.9 t DM ha^{-1}) compared to other studies which found 8.3–19.6 t DM ha^{-1} in the east of UK (Beale & Long, 1997; Christian et al., 2008; Kalinina et al., 2017; Lewandowski et al., 2003) and 14.5–25.8 t DM ha^{-1} in Croatia (Bilandžija et al., 2018, 2021; Voća et al., 2021). Reasons for this are, in the case of the UK, differences in summer temperature, soil conditions and planting density and, for Croatia, differences in soil structure and cutting height. At the Italian site, the *M × g* yield was 9.3 t DM ha^{-1}, which is substantially lower than yields found by other studies in Italy, however, with a considerably higher planting density (Alexopoulou et al., 2015; Cosentino et al., 2007). Here an unusually heavy snowstorm in December led to breaking off of stem tops and caused severe lodging. Before this event, the December yield was estimated at 16.7 t DM ha^{-1}, which is in the yield range published by Alexopoulou et al. (2015) and Cosentino et al. (2007). At the German location, despite the higher altitude, *M × g* achieved an aboveground yield of 15.7 t DM ha^{-1}, which is comparable to yields reported for a third-year crop in other studies conducted in Germany (Gauder et al., 2012; Iqbal et al., 2015; Kalinina et al., 2017; Kiesel, Nunn, et al., 2017; Lewandowski et al., 2003; Schorling et al., 2015). Detailed analysis of the year-one-to-three yield is the subject of Awty-Carrol et al. (2022).

The average N and K content levels found in this study across all four sites and hybrids were 3.3 $mg\,N\,g^{-1}$ and 5.6 $mg\,K\,g^{-1}$ at the commercial, standard delayed harvest in spring. In their review, Cadoux et al. (2012) reported slightly higher mean contents for overwinter ripened aboveground $M \times g$ biomass of 4.9 $mg\,N\,g^{-1}$ and 7 $mg\,K\,g^{-1}$ for sites located throughout Europe. Taking the average across all hybrids, we found by far the highest N and K content at the site in the UK (7.5 $mg\,N\,g^{-1}$, 9.1 $mg\,K\,g^{-1}$), followed by Germany (2.4 $mg\,N\,g^{-1}$, 6.3 $mg\,K\,g^{-1}$), Italy (1.9 $mg\,N\,g^{-1}$, 3.7 $mg\,K\,g^{-1}$), and Croatia (1.1 $mg\,N\,g^{-1}$, 3.2 $mg\,K\,g^{-1}$). The biomass from the German, Italian, and Croatian sites had N contents within the range found by various other studies (Bilandzija et al., 2017; Nassi o Di Nasso et al., 2011; Strullu et al., 2011) but both lower N and K contents than reported by Iqbal and Lewandowski (2014) and Kahle et al. (2001) for Germany. In the UK, the N content is higher and K content lower than the values found by Beale and Long (1997). The different nutrient levels reported in the literature may possibly be explained by the fact that nutrient content of harvested biomass is, to a certain extent, affected by soil nutrient availability (Kludze et al., 2013; Roncucci et al., 2015; Strullu et al., 2011). However, a correlation between soil and biomass nutrient contents was not found in this study. In the UK, the field trial was established on former grassland, which could have affected N availability by increased mobilization, but also the later ripening compared to the other locations contributed to higher nitrogen contents for all hybrids and to higher K contents for the late-ripening hybrids due to incomplete relocation.

4.2 | Seasonal dynamics of yield, nutrient contents, and stocks

In this study, the mean biomass losses over all hybrids from *peak yield* to spring harvest were 26% in Croatia, 31% in Germany, 33% in the UK, and 52% in Italy (from peak yield until December: 24%). Except for Italy, these figures are within the typical range (20%–35%) for a delayed harvest in spring (Clifton-Brown & Lewandowski, 2002; Kalinina et al., 2017; Lewandowski & Heinz, 2003; Nassi o Di Nasso et al., 2011; Strullu et al., 2011). Biomass losses were higher in Italy than at the other three locations due to the early reaching of peak yield and thus longer exposure to the weather, but were still within the range found by Bilandžija et al. (2021) for $M \times g$ in Croatia. Lodging affected the yield in two ways: first by preventing leaf-fall in completely lodged plants, resulting in a higher leaf share at harvest, and second by increased losses during harvest due to broken stems. The latter also occurred in non-lodging hybrids where stem tops were broken and lost. Of

the four hybrids, *M sin × sin* was most vulnerable to lodging. It has the thinnest stems, the highest planting density and a higher leaf share than the other hybrids. Nazli and Lewandowski (2011) also observed higher vulnerability to lodging in hybrids with thinner stems. For commercial harvests, lodging is a non-optimal scenario. Compared to a standing crop, it is much more difficult to collect the biomass and the lying biomass dries more slowly. This increases working time and costs involved in harvesting, decreases biomass quality and increases on-field biomass losses during harvest. For locations with a high risk of (early) snowfall and elevated locations prone to storm events over winter, hybrids with solid stems, early leaf-fall and thus, in total, a lower risk of lodging would appear more suitable. The yields recorded in this study were significantly influenced by G × E interactions ($p = 0.015$), with location ($p < 0.001$) having a larger effect than hybrid ($p = 0.005$). We found a quantitative and temporal gradient in the average peak yield over all hybrids per site from south to north, with the exception of ZAG. Peak yields were higher and were reached earlier the more southerly the location. It is well known that climatic conditions impact biomass yield. As a C_4 crop, miscanthus generally profits from elevated temperatures and extended growth periods under south European conditions, if the water supply is sufficient (Clifton-Brown et al., 2000).

The seasonal time courses of *nutrient contents* in the aboveground biomass show a high level (25.4 $mg\,N\,g^{-1}$) at the beginning of the growing season, followed by a sharp decline during the growing season (3.3 $mg\,N\,g^{-1}$) due to the growth dilution effects. We found significant effects of G, E, and G × E interactions on the nutrient content. Genetic differences between the N contents were relatively high, except in Italy, with higher contents for late-ripening hybrids. Lodging did not affect the nutrient content directly, but indirectly through the higher leaf share at harvest. However, in Germany and Italy, the N contents were comparatively low despite the high leaf share. The nutrient content courses indicate that the translocation of K is determined earlier than that of N. Thus, harvesting after the completion of the annual lifecycle is fundamental to achieving a low nutrient content.

The *nutrient stock*—equivalent to the nutrient offtake by the harvested biomass—was found to increase with the growth of aboveground biomass from the beginning of the growing season in April/May until the peak yield, mainly between July and December depending on the hybrid and the site. Generally, once the peak yield was reached, the nutrient stocks decreased gradually until spring harvest. Other studies also found similar time courses for nutrient stock changes for $M \times g$ (Beale & Long, 1997 in the UK; Heaton et al., 2009 in the US; Nassi o Di Nasso et al., 2011 in Italy). The nutrient stocks determined in this study

at spring harvest ranged between 6–75 kg N ha⁻¹ (mean 32.5 kg N ha⁻¹) and 15–170 kg K ha⁻¹ (mean 62 kg K ha⁻¹). Nutrient stocks found by Christian et al. (2008) and Nassi o Di Nasso et al. (2011) are within the range of the results of this study. At the beginning of the vegetation period, the nutrient stock is mainly affected by nutrient content. While the nutrient content decreases due to the dilution effect caused by increasing accumulation of organic biomass over the course of the vegetation period (Beale & Long, 1997), the nutrient stocks are primarily influenced by the time of ripening and the biomass yield. This results in higher nutrient offtakes by the harvested biomass of later-ripening and higher-yielding hybrids. Nutrient offtake at spring harvest was mainly affected by site conditions: sites with insufficient degree days for the crop to complete its annual lifecycle generally showed higher offtakes than more southerly locations with a higher number of degree days and thus a complete crop cycle. To increase yield and simultaneously minimize nutrient offtakes, late-ripening hybrids should mainly be selected for locations with relatively long vegetation periods, for example, southern Europe. At sites with a short vegetation period and lower summer temperatures, such as northern Europe, early-ripening hybrids can achieve high yields and, at the same time, minimize nutrient offtakes by the harvested biomass.

4.3 | Senescence and translocation of nutrients

In this study, the N content declined by 86% and the K content by 83% from the maximum stock until harvest. These nutrient reduction rates are in line with values found by other studies (Beale & Long, 1997; Himken et al., 1997; Nassi o Di Nasso et al., 2011; Strullu et al., 2011). As in the literature (Beale & Long, 1997; Heaton et al., 2009; Himken et al., 1997; Nassi o Di Nasso et al., 2011), we found a lower reduction in K than N content with a more distinct decline in both N and K contents at southern than at northern sites. Lewandowski et al. (2003) reported the same observation for N. This relates to a delayed ripening at northern locations.

Senescence initiates the active and passive nutrient translocation. The chloroplasts in the leaves are dissembled and stored nutrients are translocated to the seed and/ or storage organs (active translocation) (Himelblau & Amasino, 2001). Completely senescent leaves fall off (passive translocation). Leaf senescence started at the end of September at all sites. The stage at which all leaves had turned brown was found to coincide with the minimum temperature falling below −6°C at all locations. This was the earliest at the Croatian site, followed by Germany and

Italy. The assumption of Purdy et al. (2015) that the decrease in green leaves is triggered by day length and the rate of decline is driven by temperature would thus seem not only valid for *M* × *g*, but also reasonable for *M sin* × *sin* and *M sac* × *sin*. Another trigger for the start of active senescence could be the onset of flowering. However, the relationship between flowering and senescence in miscanthus has not been well defined (Jensen et al., 2017). We did not observe a direct effect of flowering on nutrient content. It is possible that the drought in September and October 2020 at the Italian site may have delayed flowering.

The physiologically *active translocation* of nutrients from the leaves and shoots to the rhizomes can be terminated by the first severe frost in late autumn or during winter, depending on the climate, killing the aboveground biomass (Clifton-Brown et al., 2001; Iqbal & Lewandowski, 2014; Strullu et al., 2011). However, at the UK site, with the mildest winters of the four locations, the hourly minimum temperature of −4.1°C was not cold enough to kill the aboveground stem biomass and thus terminate active senescence. This is consistent with Irvine (1977), who determined that *M sin* has a higher frost tolerance than sugar cane and that lethal temperatures for sugarcane range from −3.3 to −3.9°C for old leaves, −4.4 to −5.0°C for the upper stems, and −5.0 to −5.6°C for the lower stems. In addition, the canopy in dense plant stands prevents cooling and can result in temperatures up to 3.3°C higher than outside the stand (Irvine, 1977). This indicates that a single night of frost with temperatures falling to −6 to −8°C is not sufficient to completely kill all stems in a stand. However, several days of permanent frost with such temperatures would probably suffice. We found that the N content in stems was generally constant after a frost below −7.4 to −9°C and in leaves below −4°C. Compared with the other three locations, N content remained significantly higher in the UK, reflecting lower active translocation efficiency and/or a lower dilution effect due to lower biomass yields. While the K contents of the early- and medium-ripening hybrids reached the level of the German site, the late-ripening seed-based hybrid *M sac* × *sin* (GRC 14) still remobilized 20% of the K content from December to spring harvest, indicating that shoots of this late-ripening hybrid were not killed by frost over the winter. In addition, physiological maturity appears to have been delayed by the extremely late peak in nutrient stocks, and senescence was initiated relatively late in November. In contrast, the rhizome-based *M sac* × *sin* (GRC 15) was unable to take advantage of the mild winter to further reduce K levels. Although we cannot exclude site-specific effects of nutrient availability on N and K content, there is a clear trend towards higher contents in the crop of later-ripening hybrids (*M sac* × *sin*) that remain

green in the autumn at colder sites (fewer degree days). Similar to other studies (Bilandzija et al., 2017; Iqbal & Lewandowski, 2014; Magenau et al., 2021), we did not find that *leaching* has an effect on the nutrient content.

Reduction of peak N stock until harvest through biomass losses (*passive translocation*) generally accounted for 51% of the decrease. In climates with a short vegetation period and low number of degree days, large amounts of the nutrients were recycled through passive nutrient translocation. In warmer climates, where the miscanthus has enough time to finish the growth cycle, passive translocation has only a minor effect because the plant has enough time to actively translocate nutrients to the rhizomes.

5 | CONCLUSION

This study provides underlying data for the appropriate selection of high-yielding and low-offtake miscanthus hybrids with variable harvest times across a broad range of European climates. These data are needed to guide the choice of hybrid and the timing of harvests for particular locations with wide-reaching impacts on the environmental and economic sustainability of biomass production from miscanthus. The novel, early-flowering *M sin × sin* hybrid ripened more quickly than the later-flowering *M sac × sin* hybrids. As expected, this resulted in lower nutrient contents in the *M sin × sin* hybrid than in the *M sac × sin* hybrids from peak yield in September until spring harvest. This widens the harvest window—the period of time in which harvests fulfil criteria of quantity, quality, and environmental sustainability (minimal nutrient offtakes). The data presented here can also be used to provide information on and update current quality criteria by matching the biomass to logistical and end-use chains. At warmer locations, the *M sin × sin* yields were lower than those of the *M sac × sin* hybrids. The *M sin × sin* hybrids, which were planted at double the planting densities of *M sac × sin* hybrids, reached ceiling yields more quickly in northern locations, but in southern locations the *M sac × sin* hybrids planted at the lower density achieved higher yields and, at the same time, minimal nutrient offtakes. The cultivation of late-ripening miscanthus hybrids at high-latitude or high-altitude European locations is likely to increase nutrient inputs, thus reducing the overall biomass sustainability. Particularly in locations where hybrids do not actively senesce before autumn/early winter, frosts may kill the shoots, preventing active nutrient translocation to the rhizome. However, even at locations with mild winters, the continuing nutrient translocation over winter cannot fully compensate for low summer temperatures. While early-ripening *M sin × sin* had low nutrient contents, this is concomitant with low yields in warmer locations. Interestingly, the commercial *M × g*—a naturally occurring *M sac × sin* hybrid—manages to strike a good balance between high yield and quality in a wide range of locations. Breeders need to continue exploring a much larger number of *M sac × sin* hybrids to find those that combine the positive traits found in *M × g* with scalability through seed propagation and additional traits conferring increased resilience to abiotic stresses associated with extreme weather events caused by climate change.

CONFLICT OF INTEREST
The authors declare no conflict of intrest.

ORCID
Elena Magenau https://orcid.org/0000-0003-3859-9402
John Clifton-Brown https://orcid.org/0000-0001-6477-5452
Danny Awty-Carroll https://orcid.org/0000-0001-5855-0775
Andrea Ferrarini https://orcid.org/0000-0001-9390-7004
Mislav Kontek https://orcid.org/0000-0001-9042-5499
Enrico Martani https://orcid.org/0000-0003-0236-0328
Stefano Amaducci https://orcid.org/0000-0002-6184-9257
Vanja Jurišić https://orcid.org/0000-0002-4071-8637
Luisa M. Trindade https://orcid.org/0000-0003-1541-2094
Iris Lewandowski https://orcid.org/0000-0002-0388-4521
Andreas Kiesel https://orcid.org/0000-0003-0806-2532

REFERENCES

Alexopoulou, E., Zanetti, F., Scordia, D., Zegada-Lizarazu, W., Christou, M., Testa, G., Cosentino, S. L., & Monti, A. (2015). Long-term yields of switchgrass, giant reed, and *Miscanthus* in the Mediterranean Basin. *Bioenergy Research*, *8*, 1492–1499. https://doi.org/10.1007/s12155-015-9687-x

Awty-Carroll, D., Magenau, E., Al Hassan, M., Martani, E, Kontek, M., van der Pluijm, P., Ashman, C., de Maupeou, E., McCalmont, J. P., Davey, C. L., van der Cruijsen, K., Jurišić, V., Amaducci, S., Lamy, I., Kam, J., Hoogedam, A., Dolstra, O., Ferrarini, A., Lewandowski, I., ... Clifton-Brown, J. (2022). Yield performance of fourteen novel inter- and intra-species *Miscanthus* hybrids across Europe (Unpublished manuscript). Institute of Biological, Environmental and Rural Sciences, Aberystwyth University.

Beale, C. V., & Long, S. P. (1997). Seasonal dynamics of nutrient accumulation and partitioning in the perennial C_4-grasses *Miscanthus × giganteus* and *Spartina cynosuroides*. *Biomass and Bioenergy*, *12*, 419–428. https://doi.org/10.1016/S0961-9534(97)00016-0

Bilandžija, D., Bilandžija, N., & Zgorelec, Ž. (2021). Sequestration potential of energy crop *Miscanthus × giganteus* cultivated in continental part of Croatia. *Journal of Central European Agriculture*, *22*(1), 188–200. https://doi.org/10.5513/JCEA01/22.1.2776

Bilandzija, N., Jurisic, V., Voca, N., Leto, J., Matin, A., Sito, S., & Kricka, T. (2017). Combustion properties of *Miscanthus × giganteus* biomass – Optimization of harvest time. *Journal of the Energy Institute*, *90*, 528–533. https://doi.org/10.1016/j.joei.2016.05.009

Bilandžija, N., Voća, N., Leto, J., Jurišić, V., Grubor, M., Matin, A., Geršić, A., & Krička, T. (2018). Yield and biomass composition of *Miscanthus × giganteus* in the mountain area of Croatia. *Transactions of famena*, *42*, 51–60. https://doi.org/10.21278/TOF.42Si105

Buchanan-Wollaston, V., Earl, S., Harrison, E., Mathas, E., Navabpour, S., Page, T., & Pink, D. (2003). The molecular analysis of leaf senescence-a genomics approach. *Plant Biotechnology Journal*, *1*, 3–22. https://doi.org/10.1046/j.1467-7652.2003.00004.x

Cadoux, S., Riche, A. B., Yates, N. E., & Machet, J.-M. (2012). Nutrient requirements of *Miscanthus × giganteus*: Conclusions from a review of published studies. *Biomass and Bioenergy*, *38*, 14–22. https://doi.org/10.1016/j.biombioe.2011.01.015

Chen, C.-L., van der Schoot, H., Dehghan, S., Alvim Kamei, C. L., Schwarz, K.-U., Meyer, H., Visser, R. G. F., & van der Linden, C. G. (2017). Genetic diversity of salt tolerance in *Miscanthus*. *Frontiers in Plant Science*, *8*, 187. https://doi.org/10.3389/fpls.2017.00187

Christian, D. G., Riche, A. B., & Yates, N. E. (2008). Growth, yield and mineral content of *Miscanthus × giganteus* grown as a biofuel for 14 successive harvests. *Industrial Crops and Products*, *28*, 320–327. https://doi.org/10.1016/j.indcrop.2008.02.009

Clifton-Brown, J., Long, S. P., & Jørgensen, U. (2000). *Miscanthus* productivity. In M. Jones & M. Walsh (Eds.), *Miscanthus: For energy and fibre* (1st ed., pp. 46–67). Routledge.

Clifton-Brown, J. C., & Lewandowski, I. (2002). Screening *Miscanthus* genotypes in field trials to optimise biomass yield and quality in Southern Germany. *European Journal of Agronomy*, *16*, 97–110. https://doi.org/10.1016/S1161-0301(01)00120-4

Clifton-Brown, J. C., Lewandowski, I., Andersson, B., Basch, G., Christian, D. G., Kjeldsen, J. B., Jørgensen, U., Mortensen, J. V., Riche, A. B., Schwarz, K.-U., Tayebi, K., & Teixeira, F. (2001). Performance of 15 genotypes at five sites in Europe. *Agronomy Journal*, *93*, 1013–1019. https://doi.org/10.2134/agronj2001.9351013x

Cosentino, S. L., Patanè, C., Sanzone, E., Copani, V., & Foti, S. (2007). Effects of soil water content and nitrogen supply on the productivity of *Miscanthus × giganteus* Greef et Deu. in a Mediterranean environment. *Industrial Crops and Products*, *25*, 75–88. https://doi.org/10.1016/j.indcrop.2006.07.006

Cristian, D., Poulton, P., Riche, A., Yates, N. E., & Todd, A. (2006). The recovery over several seasons of ^{15}N-labelled fertilizer applied to *Miscanthus × giganteus* ranging from 1 to 3 years old. *Biomass and Bioenergy*, *30*, 125–133. https://doi.org/10.1016/j.biombioe.2005.11.002

Eichert, T., & Fernández, V. (2012). Uptake and release of elements by leaves and other aerial plant parts. In P. Marschner (Ed.), *Marschner's mineral nutrition of higher plants* (3rd ed., pp. 71–84). Elsevier.

Eisenhart, C. (1947). The assumptions underlying the analysis of variance. *Biometrics*, *3*, 1–21. https://doi.org/10.2307/3001534

Ezaki, B., Nagao, E., Yamamoto, Y., Nakashima, S., & Enomoto, T. (2008). Wild plants, *Andropogon virginicus* L. and *Miscanthus sinensis* Anders, are tolerant to multiple stresses including aluminum, heavy metals and oxidative stresses. *Plant Cell Reports*, *27*, 951–961. https://doi.org/10.1007/s00299-007-0503-8

Ferrarini, A., Fornasier, F., Serra, P., Ferrari, F., Trevisan, M., & Amaducci, S. (2017). Impacts of willow and miscanthus bioenergy buffers on biogeochemical N removal processes along the soil-groundwater continuum. *GCB Bioenergy*, *9*, 246–261. https://doi.org/10.1111/gcbb.12340

Ferrarini, A., Serra, P., Almagro, M., Trevisan, M., & Amaducci, S. (2017). Multiple ecosystem services provision and biomass logistics management in bioenergy buffers: A state-of-the-art review. *Renewable and Sustainable Energy Reviews*, *73*, 277–290. https://doi.org/10.1016/j.rser.2017.01.052

Gauder, M., Graeff-Hönninger, S., Lewandowski, I., & Claupein, W. (2012). Long-term yield and performance of 15 different *Miscanthus* genotypes in southwest Germany. *The Annals of Applied Biology*, *160*, 126–136. https://doi.org/10.1111/j.1744-7348.2011.00526.x

Gołąb-Bogacz, I., Helios, W., Kotecki, A., Kozak, M., & Jama-Rodzeńska, A. (2021). Content and uptake of ash and selected nutrients (K, Ca, S) with biomass of *Miscanthus × giganteus* depending on nitrogen fertilization. *Agriculture*, *11*, 76. https://doi.org/10.3390/agriculture11010076

Heaton, E. A., Dohleman, F. G., & Long, S. P. (2009). Seasonal nitrogen dynamics of *Miscanthus × giganteus* and *Panicum virgatum*. *GCB Bioenergy*, *1*, 297–307. https://doi.org/10.1111/j.1757-1707.2009.01022.x

Himelblau, E., & Amasino, R. M. (2001). Nutrients mobilized from leaves of *Arabidopsis thaliana* during leaf senescence. *Journal of Plant Physiology*, *158*(10), 1317–1323. https://doi.org/10.1078/0176-1617-00608

Himken, M., Lammel, J., Neukirchen, D., Czypionka-Krause, U., & Olfs, H.-W. (1997). Cultivation of *Miscanthus* under West European conditions: Seasonal changes in dry matter production, nutrient uptake and remobilization. *Plant and Soil*, *189*, 117–126. https://doi.org/10.1023/A:1004244614537

Iqbal, Y., Gauder, M., Claupein, W., Graeff-Hönninger, S., & Lewandowski, I. (2015). Yield and quality development comparison between miscanthus and switchgrass over a period of 10 years. *Energy*, *89*, 268–276. https://doi.org/10.1016/j.energy.2015.05.134

Iqbal, Y., & Lewandowski, I. (2014). Inter-annual variation in biomass combustion quality traits over five years in fifteen *Miscanthus* genotypes in south Germany. *Fuel Processing Technology*, *121*, 47–55. https://doi.org/10.1016/j.fuproc.2014.01.003

Irvine, J. E. (1977). Identification of cold tolerance in *Saccharum* and related genera through refrigerated freeze screening. In ISSCT (Ed.), *Proceedings of the 16th congress of the international society of sugar cane technologists* (pp. 147–156).

Jensen, E., Robson, P., Farrar, K., Thomas Jones, S., Clifton-Brown, J., Payne, R., & Donnison, I. (2017). Towards *Miscanthus* combustion quality improvement: The role of flowering and senescence. *Global Change Biology. Bioenergy*, *9*, 891–908. https://doi.org/10.1111/gcbb.12391

Kahle, P., Beuch, S., Boelcke, B., Leinweber, P., & Schulten, H.-R. (2001). Cropping of *Miscanthus* in Central Europe: Biomass production and influence on nutrients and soil organic matter. *European Journal of Agronomy*, *15*, 171–184. https://doi.org/10.1016/S1161-0301(01)00102-2

Kalinina, O., Nunn, C., Sanderson, R., Hastings, A. F. S., van der Weijde, T., Ozguven, M., Tarakanov, I., Schule, H., Trindade, L. M., Dolstra, O., Schwarz, K.-U., Iqbal, Y., Kiesel, A., Mos, M., Lewandowski, I., & Clifton-Brown, J. C. (2017). Extending *Miscanthus* cultivation with novel germplasm at six contrasting sites. *Frontiers in Plant Science*, *8*, 563. https://doi.org/10.3389/fpls.2017.00563

Kiesel, A. (2020). *The potential of Miscanthus as biogas feedstock* (Dissertation, University of Hohenheim).

Kiesel, A., & Lewandowski, I. (2017). *Miscanthus* as biogas substrate - cutting tolerance and potential for anaerobic digestion. *GCB Bioenergy*, *9*, 153–167. https://doi.org/10.1111/gcbb.12330

Kiesel, A., Nunn, C., Iqbal, Y., van der Weijde, T., Wagner, M., Özgüven, M., Tarakanov, I., Kalinina, O., Trindade, L. M., Clifton-Brown, J., & Lewandowski, I. (2017). Site-specific management of *Miscanthus* genotypes for combustion and anaerobic digestion: A comparison of energy yields. *Frontiers in Plant Science*, *8*, 347. https://doi.org/10.3389/fpls.2017.00347

Kiesel, A., Wagner, M., & Lewandowski, I. (2017). Environmental performance of miscanthus, switchgrass and maize: Can C_4 perennials increase the sustainability of biogas production? *Sustainability*, *9*, 5. https://doi.org/10.3390/su9010005

Kludze, H., Deen, B., & Dutta, A. (2013). Impact of agronomic treatments on fuel characteristics of herbaceous biomass for combustion. *Fuel Processing Technology*, *109*, 96–102. https://doi.org/10.1016/j.fuproc.2012.09.043

Lask, J., Magenau, E., Ferrarini, A., Kiesel, A., Wagner, M., & Lewandowski, I. (2020). Perennial rhizomatous grasses: Can they really increase species richness and abundance in arable land?—A meta-analysis. *GCB Bioenergy*, *12*, 968–978. https://doi.org/10.1111/gcbb.12750

Lewandowski, I., Clifton-Brown, J., Kiesel, A., Hastings, A., & Iqbal, Y. (2018). *Miscanthus*. In E. Alexopoulou (Ed.), *Perennial grasses for bioenergy and bioproducts: Production, uses, sustainability and markets for giant reed, miscanthus, switchgrass, reed canary grass and bamboo* (pp. 35–59). Academic Press. https://doi.org/10.1016/B978-0-12-812900-5.00002-3

Lewandowski, I., Clifton-Brown, J., Trindade, L. M., van der Linden, G. C., Schwarz, K.-U., Müller-Sämann, K., Anisimov, A., Chen, C.-L., Dolstra, O., Donnison, I. S., Farrar, K., Fonteyne, S., Harding, G., Hastings, A., Huxley, L. M., Iqbal, Y., Khokhlov, N., Kiesel, A., Lootens, P., … Kalinina, O. (2016). Progress on optimizing *Miscanthus* biomass production for the European bioeconomy: Results of the EU FP7 Project OPTIMISC. *Frontiers in Plant Science*, *7*, 1620. https://doi.org/10.3389/fpls.2016.01620

Lewandowski, I., Clifton-Brown, J. C., Andersson, B., Basch, G., Christian, D. G., Jørgensen, U., Jones, M., Riche, A. B., Schwarz, K.-U., Tayebi, K., & Teixeira, F. (2003). Environment and harvest time affects the combustion qualities of *Miscanthus* genotypes. *Agronomy Journal*, *95*, 1274–1280. https://doi.org/10.2134/agronj2003.1274

Lewandowski, I., & Heinz, A. (2003). Delayed harvest of miscanthus—influences on biomass quantity and quality and environmental impacts of energy production. *European Journal of Agronomy*, *19*, 45–63. https://doi.org/10.1016/S1161-0301(02)00018-7

Lim, P. O., Kim, H. J., & Nam, H. G. (2007). Leaf senescence. *Annual Review of Plant Biology*, *58*, 115–136. https://doi.org/10.1146/annurev.arplant.57.032905.105316

Magenau, E., Kiesel, A., Clifton-Brown, J., & Lewandowski, I. (2021). Influence of cutting height on biomass yield and quality of miscanthus genotypes. *GCB Bioenergy*, *13*, 1675–1689. https://doi.org/10.1111/gcbb.12881

Mangold, A., Lewandowski, I., Möhring, J., Clifton-Brown, J., Krzyżak, J., Mos, M., Pogrzeba, M., & Kiesel, A. (2019). Harvest date and leaf:stem ratio determine methane hectare yield of miscanthus biomass. *GCB Bioenergy*, *11*, 21–33. https://doi.org/10.1111/gcbb.12549

Mitros, T., Session, A. M., James, B. T., Wu, G. A., Belaffif, M. B., Clark, L. V., Shu, S., Dong, H., Barling, A., Holmes, J. R., Mattick, J. E., Bredeson, J. V., Liu, S., Farrar, K., Głowacka, K., Jeżowski, S., Barry, K., Chae, W. B., Juvik, J. A., … Rokhsar, D. S. (2020). Genome biology of the paleotetraploid perennial biomass crop *Miscanthus*. *Nature Communications*, *11*, 5442. https://doi.org/10.1038/s41467-020-18923-6

Mos, M., Robson, P. R. H., Buckby, S., Hastings, A. F., Helios, W., Jama-Rodzeńska, A., Kotecki, A., Kalembasa, D., Kalembasa, S., Kozak, M., Chmura, K., Serafin-Andrzejewska, M., & Clifton-Brown, J. (2021). Seasonal dynamics of dry matter accumulation and nutrients in a mature *Miscanthus × giganteus* stand in the lower Silesia region of Poland. *Agronomy*, *11*, 1679. https://doi.org/10.3390/agronomy11081679

Nassi o Di Nasso, N., Roncucci, N., Triana, F., Tozzini, C., & Bonari, E. (2011). Seasonal nutrient dynamics and biomass quality of giant reed (*Arundo donax* L.) and miscanthus (*Miscanthus × giganteus* Greef et Deuter) as energy crops. *Italian Journal of Agronomy*, *6*, 152–158. https://doi.org/10.4081/ija.2011.e24

Naumann, C., & Bassler, R. (1976). Die chemische Untersuchung von Futtermitteln. In *Band III. Verband Deutscher Landwirtschaftlicher Untersuchungs-und Forschungsanstalten*. VDLUFA-Verlag, Darmstadt.

Nazli, R., & Lewandowski, I. (2011). Evaluation of nitrogen fertilization and genotype effects on lodging of miscanthus and switchgrass. In *19th European biomass conference and exhibition proceedings, Berlin, Germany* (pp. 619–622). ETA-Florence Renewable Energies. https://doi.org/10.5071/19thEUBCE2011-VP1.3.24

Nunn, C., Hastings, A. F. S. J., Kalinina, O., Özgüven, M., Schüle, H., Tarakanov, I. G., van der Weijde, T., Anisimov, A. A., Iqbal, Y., Kiesel, A., Khokhlov, N. F., McCalmont, J. P., Meyer, H., Mos, M., Schwarz, K.-U., Trindade, L. M., Lewandowski, I., & Clifton-Brown, J. C. (2017). Environmental influences on the growing season duration and ripening of diverse miscanthus germplasm grown in six countries. *Frontiers in Plant Science*, 8, 907. https://doi.org/10.3389/fpls.2017.00907

Pidlisnyuk, V., Stefanovska, T., Lewis, E. E., Erickson, L. E., & Davis, L. C. (2014). *Miscanthus* as a productive biofuel crop for phytoremediation. *Critical Reviews in Plant Sciences*, 33, 1–19. https://doi.org/10.1080/07352689.2014.847616

Pogrzeba, M., Rusinowski, S., Sitko, K., Krzyżak, J., Skalska, A., Małkowski, E., Ciszek, D., Werle, S., McCalmont, J. P., Mos, M., & Kalaji, H. M. (2017). Relationships between soil parameters and physiological status of *Miscanthus × giganteus* cultivated on soil contaminated with trace elements under NPK fertilisation vs. microbial inoculation. *Environmental Pollution*, 225, 163–174. https://doi.org/10.1016/j.envpol.2017.03.058

Purdy, S. J., Cunniff, J., Maddison, A. L., Jones, L. E., Barraclough, T., Castle, M., Davey, C. L., Jones, C. M., Shield, I., Gallagher, J., Donnison, I., & Clifton-Brown, J. (2015). Seasonal carbohydrate dynamics and climatic regulation of senescence in the perennial grass, *Miscanthus. Bioenergy Research*, 8, 28–41. https://doi.org/10.1007/s12155-014-9500-2

R Core Team. (2019). *R: A Language and environment for statistical computing*. R Foundation for Statistical Computing. https://www.R-project.org/

Roncucci, N., Nassi o Di Nasso, N., Tozzini, C., Bonari, E., & Ragaglini, G. (2015). *Miscanthus × giganteus* nutrient concentrations and uptakes in autumn and winter harvests as influenced by soil texture, irrigation and nitrogen fertilization in the Mediterranean. *GCB Bioenergy*, 7, 1009–1018. https://doi.org/10.1111/gcbb.12209

Rusinowski, S., Krzyżak, J., Clifton-Brown, J., Jensen, E., Mos, M., Webster, R., Sitko, K., & Pogrzeba, M. (2019). New *Miscanthus* hybrids cultivated at a polish metal-contaminated site demonstrate high stomatal regulation and reduced shoot Pb and Cd concentrations. *Environmental Pollution*, 252, 1377–1387. https://doi.org/10.1016/j.envpol.2019.06.062

Schorling, M., Enders, C., & Voigt, C. A. (2015). Assessing the cultivation potential of the energy crop *Miscanthus × giganteus* for Germany. *GCB Bioenergy*, 7, 763–773. https://doi.org/10.1111/gcbb.12170

Smith, R., & Slater, F. M. (2011). Mobilization of minerals and moisture loss during senescence of the energy crops *Miscanthus × giganteus*, *Arundo donax* and *Phalaris arundinacea* in Wales, UK. *GCB Bioenergy*, 3, 148–157. https://doi.org/10.1111/j.1757-1707.2010.01069.x

Strullu, L., Cadoux, S., Preudhomme, M., Jeuffroy, M.-H., & Beaudoin, N. (2011). Biomass production and nitrogen accumulation and remobilisation by *Miscanthus × giganteus* as influenced by nitrogen stocks in belowground organs. *Field Crops Research*, 121, 381–391. https://doi.org/10.1016/j.fcr.2011.01.005

Thomas, H., & Stoddart, J. L. (1980). Leaf senescence. *Annual Review of Plant*, 31, 83–111. https://doi.org/10.1146/annurev.pp.31.060180.000503

Voća, N., Leto, J., Karažija, T., Bilandžija, N., Peter, A., Kutnjak, H., Šurić, J., & Poljak, M. (2021). Energy properties and biomass yield of *Miscanthus × giganteus* fertilized by municipal sewage sludge. *Molecules*, 26, 4731. https://doi.org/10.3390/molecules26144371

Wagner, M., & Lewandowski, I. (2017). Relevance of environmental impact categories for perennial biomass production. *GCB Bioenergy*, 9, 215–228. https://doi.org/10.1111/gcbb.12372

Wagner, M., Mangold, A., Lask, J., Petig, E., Kiesel, A., & Lewandowski, I. (2019). Economic and environmental performance of miscanthus cultivated on marginal land for biogas production. *GCB Bioenergy*, 11, 34–49. https://doi.org/10.1111/gcbb.12567

Wickham, H. (2009). Getting started with qplot. In *ggplot2*. R. Springer. https://doi.org/10.1007/978-0-387-98141-3_2

Yates, N.E., Riche, A.B., Shield, I., Zapater, M., Ferchaud, F., Ragalini, G., & Roncucci, N. (2015). Investigating the longterm biomass yield of *Miscanthus giganteus* and switchgrass when harvested as a green energy feedstock. *23rd European biomass conference and exhibition*. Vienna, Austria.

SUPPORTING INFORMATION
Additional supporting information can be found online in the Supporting Information section at the end of this article.

How to cite this article: Magenau, E., Clifton-Brown, J., Awty-Carroll, D., Ashman, C., Ferrarini, A., Kontek, M., Martani, E., Roderick, K., Amaducci, S., Davey, C., Jurišić, V., Kam, J., Trindade, L. M., Lewandowski, I., & Kiesel, A. (2022). Site impacts nutrient translocation efficiency in intraspecies and interspecies miscanthus hybrids on marginal lands. *GCB Bioenergy*, 14, 1035–1054. https://doi.org/10.1111/gcbb.12985